

MARDIE SOLAR SALT DEVELOPMENT

COMPARISON OF INUNDATION OVER THE NORTH-EASTERN FLOODWAY WITH CONSTRUCTION OF A ROAD CAUSEWAY

Rev B

MAW0616J.005
Inundation assessment for
Causeway
0
3 April 2020

REPORT

Document status

Version	Purpose of document	Authored by	Reviewed by	Approved by	Review date
A	For internal review	SL, RA	SL		2/4/2020
0	For client review		SL	SL	3/4/2020

Approval for issue

Scott Langtry

[

3 April 2020

This report was prepared by RPS within the terms of RPS' engagement with its client and in direct response to a scope of services. This report is supplied for the sole and specific purpose for use by RPS' client. The report does not account for any changes relating the subject matter of the report, or any legislative or regulatory changes that have occurred since the report was produced and that may affect the report. RPS does not accept any responsibility or liability for loss whatsoever to any third party caused by, related to or arising out of any use or reliance on the report.

Prepared by:

Prepared for:

RPS

BC Minerals

Scott Langtry
Principal Scientist

Level 2, 27-31 Troode Street
West Perth WA 6005

T +61 8 9211 1111
E scott.langtry@rpsgroup.com

Contents

1	EXECUTIVE SUMMARY	1
2	BACKGROUND	2
3	INPUT DATA.....	1
3.1	Model framework.....	1
3.2	Topography	1
3.3	Causeway alignment, height and width	3
3.4	Specification of flow through culverts and other openings.....	4
3.5	Environmental forcing	7
3.6	Observation points - – Comparative inundation for optimum design	8
3.7	Initial testing for variations of culverts and causeway heights	9
3.8	Comparison of inundation over full spring tide for optimum design	1
4	REFERENCES	6

Figures

Figure 3.1	Digital elevation model of the north-eastern clay-pan derived by LIDAR survey. Black line represents the proposed causeways alignment. The red hashed line represents the area where algal mats have been observed.	1
Figure 3.2:	Digital elevation model defined within the model for the full model domain with differentiation of heights of land features between 1.0 and 2.4 m AHD. The box defines the focus area for this investigation, illustrated in more detail in Figure 3.3.	2
Figure 3.3:	Digital elevation model defined within the model illustrated for the focus area for this study with differentiation of heights for land features between 1.0 and 2.4 m AHD.	3
Figure 3.4:	Digital elevation model defined within the model illustrating the proposed alignment of the causeway and pond walls as pink lines. Sections 1 and 2 are referred to in Table 3-1 and the text of this report.	4
Figure 3.5	Sample tidal variation along the northern portion of the grid that was applied to the assessment. The pink box defines a period of high spring tides. The black lines bracket the period applied to initial tests and for the subsequent comparison.	8
Figure 3.6:	Design of the causeway represented by Test 22. The black lines represent sections that are 4.4. m above MSL. The green line along Section 2 represents a section along the causeway that is set at 2.5 m MSL. Elsewhere, the natural topography is preserved. Locations marked Sq. culvert have 1.5 m wide square culverts set at ground level penetrating the raised section of causeway. Observation points for water inundation (AME1-8) are plotted.	9
Figure 3.7:	Calculations for local water depth over the focus area (natural topography) during a relatively low (1.4 m) spring tide. Time differences between the images are 1 hour and then 5 hours.	1
Figure 3.8:	Calculations for local water depth over the focus area (natural topography) during a relatively high (2.2 m) spring tide following the lower tidal peak shown in Figure 3.6. Time differences between the images are 1 hour and then 5 hours.	1
Figure 3.9:	Calculations for water depth over the focus area with the causeway in place and with the opening structures specified for Test 15 (See Table 3-1) over the period of a relatively high (2.2 m) spring tide following the lower tidal peak.	2
Figure 3.10:	Calculations for water depth over the focus area with the causeway in place and with the opening structures specified for Test 22 (See Table 3-1) over the period of a relatively high (2.2 m) spring tide following the lower tidal peak.	2
Figure 3.11	Local water depth over time at AME1 comparing the Base Case (blue line) and Test 22 configuration (orange dashed line). See Figure 3.6 for location.	2

Figure 3.12 Local water depth over time at AME2 comparing the Base Case (blue line) and Test 22 configuration (orange dashed line). See Figure 3.6 for location.	2
Figure 3.13 Local water depth over time at AME3 comparing the Base Case (blue line) and Test 22 configuration (orange dashed line). See Figure 3.6 for location.	3
Figure 3.14 Local water depth over time at AME4 comparing the Base Case (blue line) and Test 22 configuration (orange dashed line). See Figure 3.6 for location.	3
Figure 3.15 Local water depth over time at AME5 comparing the Base Case (blue line) and Test 22 configuration (orange dashed line). See Figure 3.6 for location.	4
Figure 3.16 Local water depth over time at AME6 comparing the Base Case (blue line) and Test 22 configuration (orange dashed line). See Figure 3.6 for location.	4
Figure 3.17 Local water depth over time at AME7 comparing the Base Case (blue line) and Test 22 configuration (orange dashed line). See Figure 3.6 for location.	5
Figure 3.18 Local water depth over time at AME8 comparing the Base Case (blue line) and Test 22 configuration (orange dashed line). See Figure 3.6 for location.	5

Tables

Table 3-1: Combinations of water blockage and conditional openings that were tested using the inundation model	5
--	---

Appendix A

Plots showing inundation and local water depth calculated over the focus area for the Base Case and Test Cases.

1 EXECUTIVE SUMMARY

Modelling of tidal inundation under an example spring tide sequence was undertaken for the natural topography without any ponds or other infrastructure in place. The example tidal sequence was chosen to represent a period of contemporary tidal variation within inclusion of relatively high, near-extreme, peak tides. The simulation indicated that tidal water would flood out over the clay pan as a relatively shallow (20-50 cm) sheet flow during higher spring tide peaks, with the sheet flow arriving at the proposed causeway alignment just before the tide began to lower offshore and within the major creek, resulting in a short period before the tidal-head began to relax and water held up over the front of the clay-pan to begin to flow back to the creeks to the west. The sheet flow that is being driven by the tidal head must pass over a ridge of marginally-higher ground that is positioned to the east of the proposed causeway alignment, and then flows by gravity out over the clay-pan. These observations are significant because it indicates that there will be a limited period over which there would be a positive head of pressure to force water through culverts if water is held up by the causeway.

Modelling of the natural situation indicated that tidal floods will sheet out over the floodway under the momentum generated by the head of water building up offshore over flood tides. This water arrives at the alignment of the causeway relatively late in the flood-tide phase and the momentum of the flood tides over the spring tide periods is sufficient to cause inundation over the claypan beyond the causeway alignment. Simulations indicate that tidal heights as low as 1.2-1.3 m are sufficient to result in inundation of at least parts of the clay-pans supporting crusting algal mats while tidal heights approaching 1.8 m would result in inundation over all parts of the clay-pan supporting crusting algae.

Modelling of inundation where a causeway was imposed along the proposed alignment, including selective water flows representative of different configurations of drainage structures and openings indicated that designs that offered relatively low cross-sections to water flow resulted in large changes in the inundation of the clay-pan areas by stopping the momentum of the sheet flows long enough for tidal heights to drop offshore so that most of the water volume flowed back to the creeks over the ebb cycle. Build up of water volume along the causeway generated some additional head of water but the loss of momentum hindered flow over the natural ridge to the east of the causeway alignment. Higher inundation was calculated for openings that were larger and placed across the lower ground levels where water flow is greatest. Simulation of a causeway that included open bridge sections placed at the lower ground sections, resulted in water sheeting through the open sections. However, multiple bridge sections would be required to carry the volume that flows across the causeway alignment under the natural topography.

Simulation of the configuration where the causeway dropped down to natural ground level to pass over a series of 200 m long flood-ways placed at sections with lower ground levels and with supplementary drainage through box culverts resulted in the momentum of the sheet flow being maintained as the flood passed through the causeway alignment and over the natural ridge of higher ground, supporting gravity flow over the wider part of the clay-pan, wetting out a comparable area to a comparable depth to the natural configuration. Comparison of hydrographs representing local water depth at observation points within the crusting algal habitat were essentially identical for the natural case and this configuration, in terms of both the depth and the phase of the inundation patterns. These results indicate that natural inundation patterns should be maintained with this causeway configuration.

2 BACKGROUND

BC Minerals limited (BCI) is proposing to construct new solar-salt production facilities near Mardie, on the Pilbara Coast of Western Australia.

The project would involve construction of a series of linked evaporation ponds over the impermeable soils that occur inshore from the coast. The coast is composed of mud and sand banks in front of relatively flat and highly-eroded land that is penetrated by multiple, highly-branched, creeks that extend up to several kilometres inland. Clay pans occur behind the mangrove zone and a portion of the clay pan area is colonised by algae and cyanobacteria that form extensive crusting mats.

RPS has delivered a numerical assessment of inundation frequencies over the vegetated habitats that occur on the western side of the development area, comparing inundation under high spring tidal sequences, and with allowance for sea level rise to quantify any effect of the pond wall structures (RPS 2019).

Subsequently, RPS was commissioned to extend and apply the inundation model to guide the design of a road causeway that BCI have proposed building to carry product from the crystallizer pond to a new port that BCI propose to construct. The causeway would cross a clay pan area that extends some 25-30 km to the north-east, inshore of a coastal dune system. Field observations and review of satellite imagery indicated that the clay pan is extensively inundated during higher spring tides with the only inflow and outflow path being at the western end, within the development area. Consequently, construction of a raised, solid, causeway across the clay pan would block flooding and drainage of seawater exchanging with the sea and tidal creek system within the development area.

Following initial assessment of the distribution of mangrove creeks and major drainage paths, BCI identified a causeway alignment that is expected to minimise primary impacts on existing mangrove and saltmarsh habitats (habitat removal during construction, disturbance to drainage during causeway construction) while reducing the frequency at which tidal waters would reach the causeway alignment. The southern section of the road causeway was routed towards the east, traversing over sections of naturally higher ground that does not support mangrove, saltmarsh or crusting algal mats, before turning towards the north to cross the clay pan along a path that was inland from the mangrove and saltmarsh habitats.

The focus of this study was the testing of alternative drainage arrangements through the causeway with the aim of achieving water exchange that was as similar to natural inundation as possible to minimise the potential for secondary impacts to algal mats that would be upstream of the proposed causeway alignment.

This study proceeded in two stages:

1. Iterative modelling of alternative designs for the causeway height and drainage design, comparing inundation extent and drainage patterns over the clay-pan area calculated for each design against calculations for the natural topography. Short-term (2-day) simulations were completed corresponding to a sequence of (2 day) spring high tide pulses to identify the optimum design.
2. Simulation of inundation over a longer (6 day) spring tide period for the optimum design and base case, with calculation of sea-level over time at reference sites within the vegetated habitats.

Modelling of tidal inundation under an example spring tide sequence was undertaken for the natural topography without any ponds or other infrastructure in place. The example tidal sequence was chosen to represent a period of contemporary tidal variation with inclusion of relatively high peak tides that are near the extreme range for contemporary sea levels.

Twenty-one variations of drainage designs were assessed in comparison to the natural flooding. These options were defined by BCI as practical alternatives with consideration of construction and costs for the planned function of the causeway. The assessment considered variations in the number and placement of round or square culverts and alternatives of creating openings that would be spanned by trestle sections or constructed as open flood-ways (low sections at the natural ground height). Simulations were also conducted with representation of spoon drains in combination with culverts to assess for improvement in conductance of water through the causeway.

3 INPUT DATA

3.1 Model framework

Hydrodynamic modelling was conducted using the Delft3D Flow modelling framework, previously described in RPS (2019). This framework supports the calculation of water flow over permanently and intermittently submerged land due to variations in water level occurring at offshore boundaries and includes algorithms that support the representation of blocks to water flow (thin dams) in combination with restrictions of water flow (culverts) over intermittently submerged land. Culverts are specified in terms of the height of their base relative to a datum level, hence surrounding ground levels, cross-sectional area available to water flow, and drag forces presented to water flow. Culverts can be represented as features that perforate thin dams at the appropriate dimensions for the culvert specification.

As described in RPS (2019), the inundation model was configured with a nested grid arrangement, where an outer domain (outer domain) with relatively coarse specification of bathymetry was used to calculate tidal variation over time along the boundary of a finer grid (inundation domain) covering the proposed extent of the Mardie Development.

The inundation domain described in RPS (2019) was extended to cover a large portion of the clay-pan area to the north-east of the proposed causeway alignment. The spatial resolution of the grid cells over the expanded area was maintained at the same resolution as the wider part of the inundation domain (10 m x 10 m). Consequently, the topography of the ground level was horizontally-averaged over 10 m x 10 m.

3.2 Topography

The topography over the extension to the inundation domain was defined by a digital elevation model (DEM) prepared by a third-party organisation (Aerometrix), derived by LIDAR survey technology. Data was received with a spatial resolution of 10 cm following height control to correct for vegetation canopies and correct any vertical distortions to within 0.1 m based on survey measurement at ground stations. Data was at the same height datum to the DEM applied over the wider area and seamlessly extended that data without datum shift. The data also spanned the area of the clay-pans where crusting algal mats had been mapped by BCI (Figure 3.1



Figure 3.1 Digital elevation model of the north-eastern clay-pan derived by LIDAR survey. Black line represents the proposed causeways alignment. The red hashed line represents the area where algal mats have been observed.

Data was interpolated by spatial averaging over the topographic scale of the model grid (10 m x 10 m horizontally) that represented the extension to the model domain.

Topographic heights defined over the full model grid are illustrated in Figure 3.2 with local details over the north-eastern portion of the full model grid illustrated in Figure 3.3. The colour scale range covers the range 1.0 - 2.4 m AHD and the key has been set to emphasis depth variation over the range 1.0 -1.7 m AHD, which range is illustrated in shades of blue to cream.

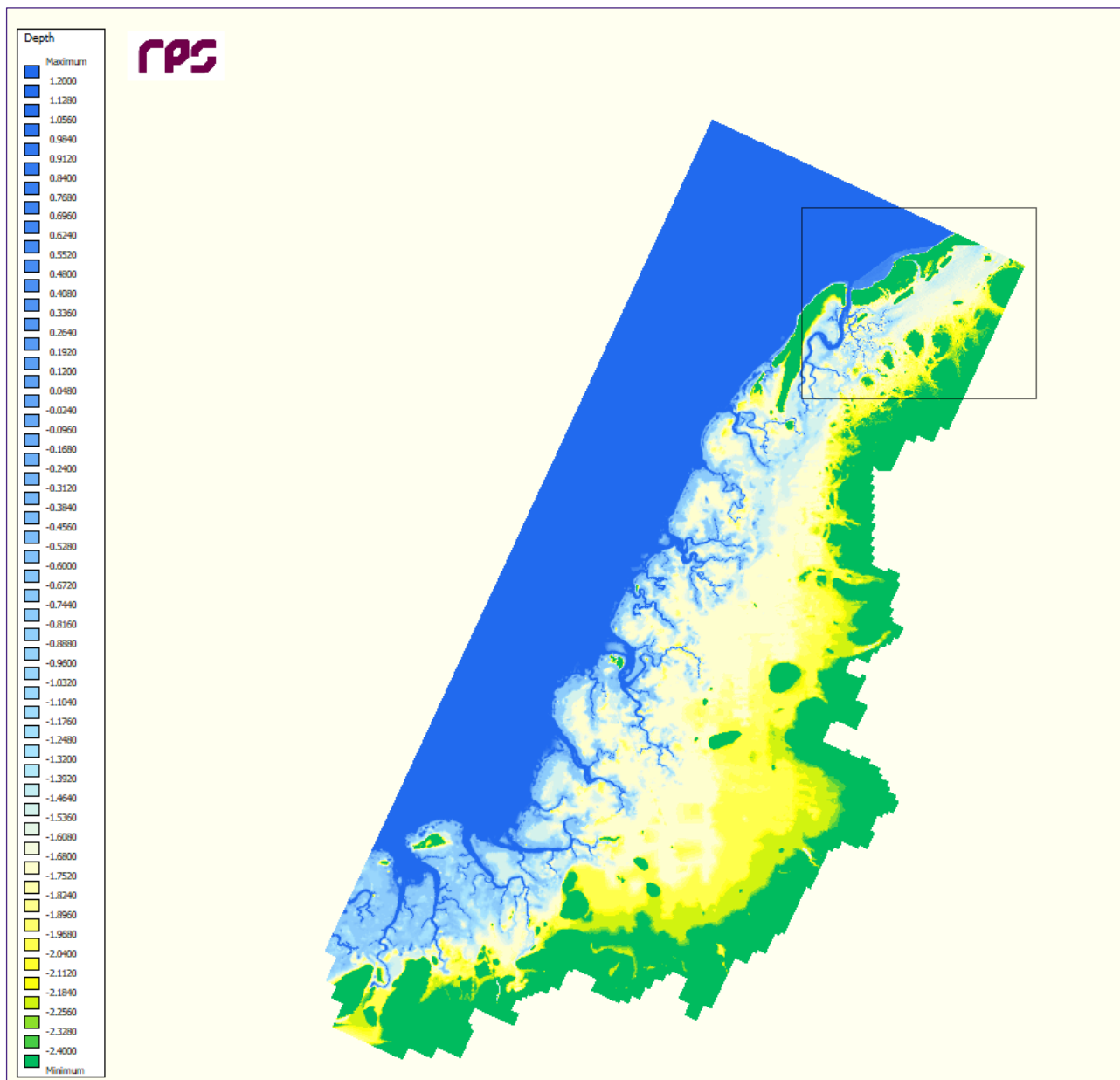


Figure 3.2: Digital elevation model defined within the model for the full model domain with differentiation of heights of land features between 1.0 and 2.4 m AHD. The box defines the focus area for this investigation, illustrated in more detail in Figure 3.3.

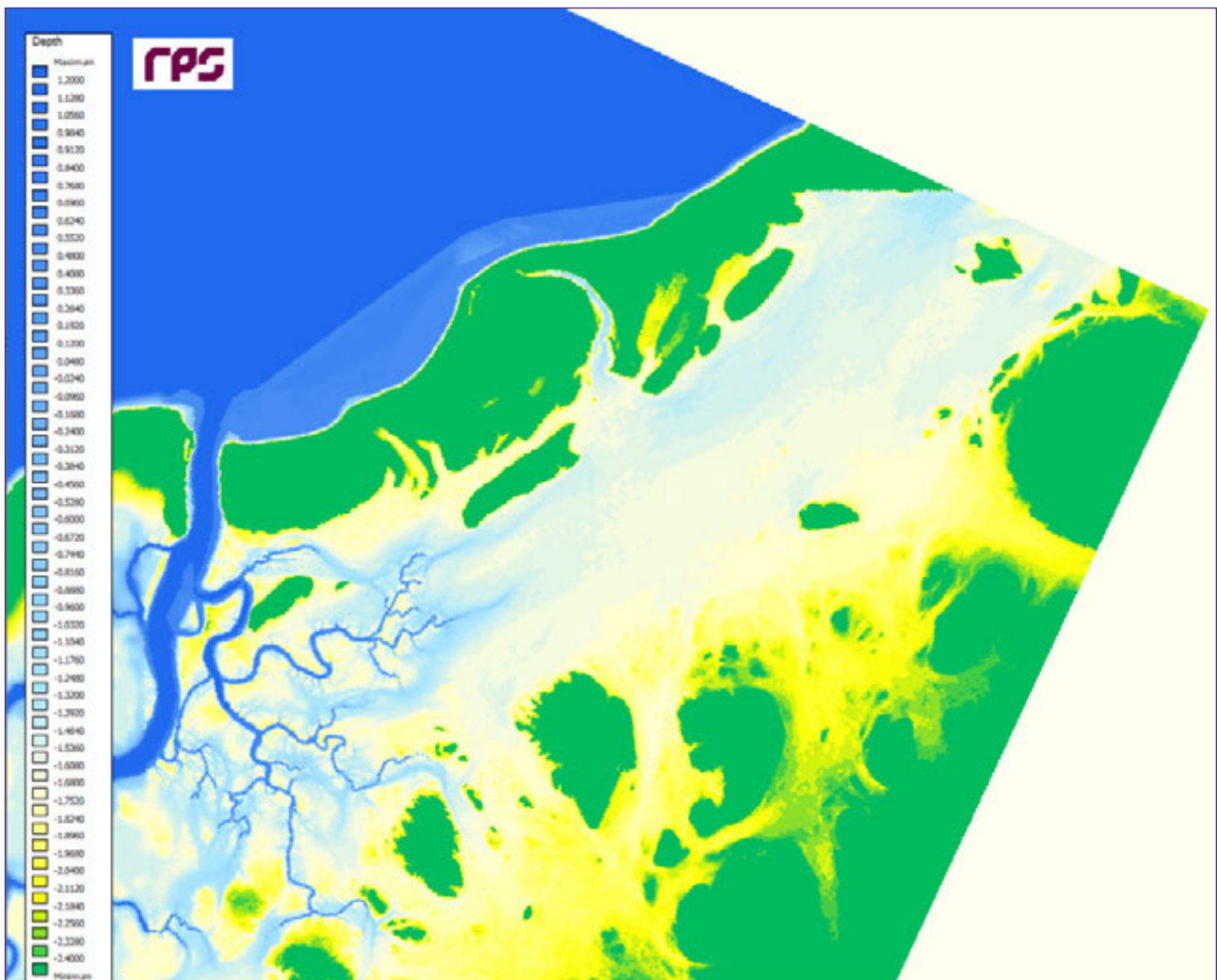


Figure 3.3: Digital elevation model defined within the model illustrated for the focus area for this study with differentiation of heights for land features between 1.0 and 2.4 m AHD.

3.3 Causeway alignment, height and width

BCI specified a proposed alignment for the causeway, which would link to the walls of the crystallizer pond and extend across a series of higher plateaus and valleys in the clay-pan to the north-east. The default height of the causeway was specified as 4.2 m above sea level, which would place the top of the causeway above any tidal level. The width of the causeway would be of the order of 10 m at the roadway, indicating a height at the base of the order of 18-20 m, allowing for a batter on the wall slopes. This information was applied to specifying the length of culverts or other openings through the culvert, for specification of drag allowance.

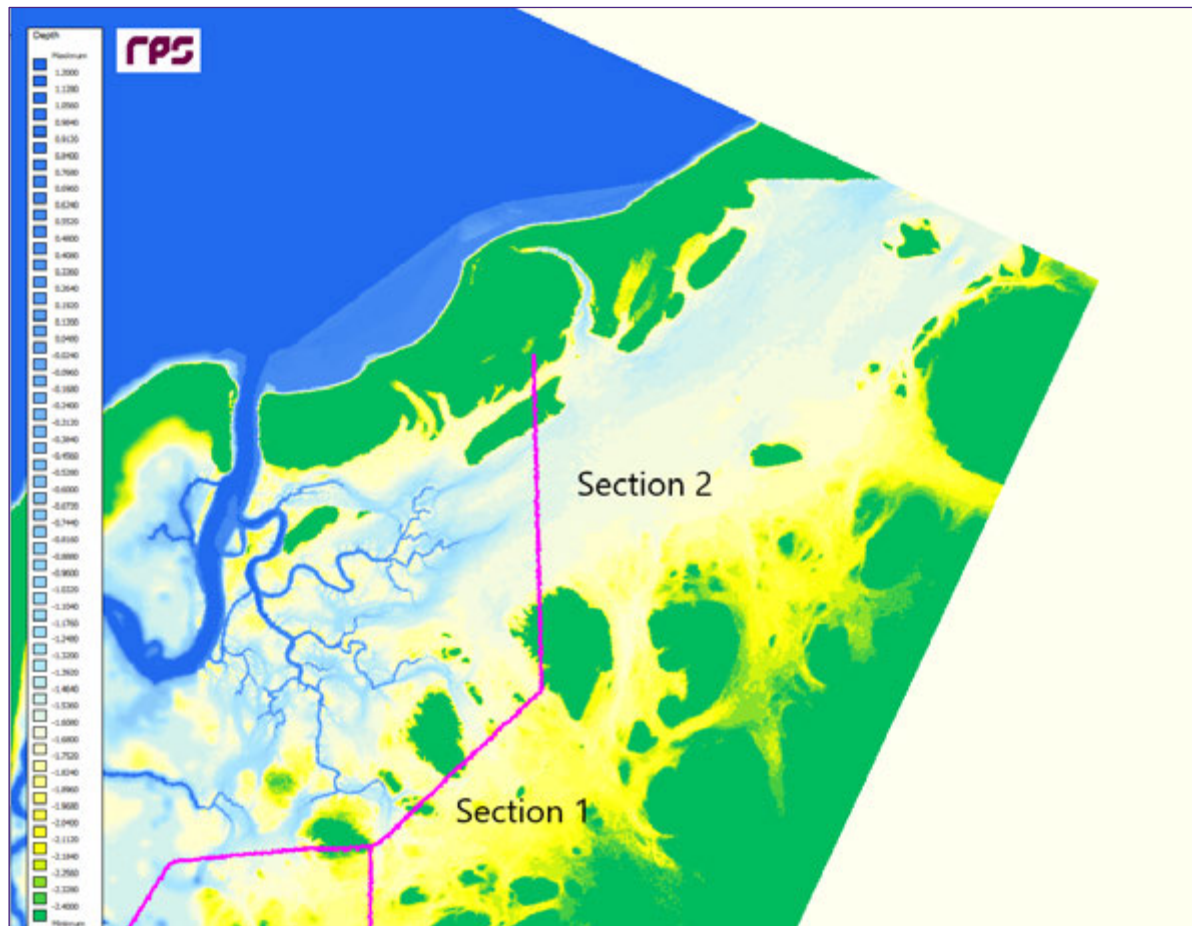


Figure 3.4: Digital elevation model defined within the model illustrating the proposed alignment of the causeway and pond walls as pink lines. Sections 1 and 2 are referred to in Table 3-1 and the text of this report.

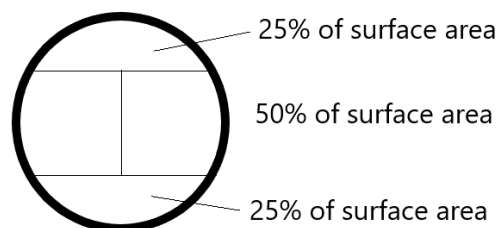
3.4 Specification of flow through culverts and other openings

The investigation assessed the inundation of seawater over the claypans for alternative designs involving the following openings through the causeway:

1. Round pipes
2. Square (box) culverts
3. Piled bridge sections
4. Flood-ways
5. Spoon-drains in association with the above structures

Openings and other structures were specified by setting the base height of the structure (or opening) and the cross-sectional area available for flow.

Round pipes will present increasing surface area for flow of water for higher water levels, commencing at the base level of the pipe-opening and with no further increase when the water level reaches the upper level of the pipe-opening. The rate of increase will increase as the water level rises to the centre-line of the pipe, and then decrease due to the circular shape of the opening. The maximum surface area available for water flow, varying with water-depth, for round pipes were represented in the model by calculating the cross-sectional area of the pipe-opening and subdividing the area into 4 sections. For example, for 600 mm round pipes (0.283 m² opening), there would be up to 0.071 m² for flow in the lower and upper 200 mm height and 0.142 m² flow in the central 400 mm.



The cross-section available for water flow through box culverts, being rectangular, were specified by width and height above base level so that no additional flow occurred if water level exceeded the culvert height. In contrast, openings for bridge sections and flood-ways were specified by width only, with no limit on increase of water flow as height increased.

Spoon-drains were specified by lowering the local topography adjacent to opening structures, with sloped applied in the upstream and downstream directions.

Structures were selectively placed along the proposed causeway alignment to maximise water flow through the causeway, given the design specifications for each variant, while also aiming to achieve similar distributions of water over the wider claypan. To this end, more of the openings allowed for under each variant were concentrated along sections that had lower ground levels and should receive higher flows at lower tide levels, as well as higher peak flows. These placements were guided by simulation of the natural inundation and by erosion patterns observable in satellite images. Additional openings were placed at sections where the natural ground level was higher to maintain direct through-put of water to locations that would be inundated to lower depths, or less frequently, without relying on the spread of water that inundates through lower sections.

The following options were tested (Table).

Table 3-1: Combinations of water blockage and conditional openings that were tested using the inundation model

Test	Detail	Culvert or opening types	Number of openings
Base Case	Natural topography	None	NA
2	Causeway penetrated by pipes at natural ground level	Pipes (600 mm D.)	68 (at 32 centres)
3	Causeway penetrated by pipes at natural ground level along all Sections	Pipes (600 mm D.)	136 (at 32 centres)
4	Causeway with open bridge sections (200 m, 30 m and 10 m long) along Section 2. Causeway with 10 m open sections along Section 1	200 m and 30 m bridges over major flow-ways with 10 m bridges regularly placed elsewhere	2 @ 200 m (Section 2) 7 @ 30 m (Section 2) 10 @ 10 m (Section 2) 20 @ 10 m (Section 1)
5	Causeway penetrated by box culverts along all Sections, concentrated at low sections,	Box culverts (500 mm W x 1200 mm H)	206 (at 90 centres)

REPORT

	with increased number over Test 3		
6	Test 4 with addition of trenches along the length of the Sections, on upstream and downstream side	200 m and 30 m bridges over major flow-ways with 10 m bridges regularly placed elsewhere	2 @ 200 m (Section 2) 7 @ 30 m (Section 2) 15 @ 10 m (Section 2) 15 @ 10 m (Section 1)
7	Causeway penetrated by wider box culverts than Test 5	Box culverts (1200 mm W x 1500 mm H)	138
8	Test 7 with increased number of box culverts	Box culverts (1200 mm W x 1500 mm H)	207
9	Test 8 with increased number of box culverts	Box culverts (1200 mm W x 1500 mm H)	276
10	Test 7 with local drain on both sides of culverts. Drains at 500 mm below local height.	Box culverts (1200 mm W x 1500 mm H)	138
11	Test 10 with increased number of box culverts	Box culverts (1200 mm W x 1500 mm H)	207
12	Test 11 with increased number of box culverts	Box culverts (1200 mm W x 1500 mm H)	276
13	Causeway penetrated by 2 m wide box culverts at regular 15 m centres along Section 2. Causeway penetrated by 1.2 m wide box culverts along Section 1.	Combination of box culverts (1200 mm W x 1500 mm H) and 2000 mm W x 1500 mm H)	25 @ 2000 mm @ 15 m centres (Section 2). 68 @ 1200 mm (Section 1 and 2)
14	Test 13 with additional 1200 mm box culverts	Combination of Box culverts (1200 mm W x 1500 mm H) and 2000 m W x 1500 mm H)	25 @ 2000 mm @ 15 m centres (Section 2). 102 @ 1200 mm (Section 1 and 2)
15	Test 14 with additional 1200 mm box culverts	Combination of Box culverts (1200 mm W x 1500 mm H) and 2000 m W x 1500 mm H)	25 @ 2000 mm @ 15 m centres (Section 2). 136 @ 1200 mm (Section 1 and 2)
16	Test 7 with lowering of plateau at north and opening	Box culverts (1200 mm W x 1500 mm H)	138 @ 1200 mm (Section 1 and 2)

of a drainage channel to the sea at 1.5 m MSL

17	Test 13 with lowering of plateau at north and opening of a drainage channel to the sea at 1.5 m MSL	Combination of box culverts (1200 mm W x 1500 mm H) and 2000 mm W x 1500 mm H)	25 @ 2000 mm @ 15 m centres (Section 2). 68 @ 1200 mm (Section 1 and 2)
18	Test 15 with local spoon drains	Combination of Box culverts (1200 mm W x 1500 mm H) and 2000 m W x 1500 mm H)	25 @ 2000 mm @ 15 m centres (Section 2). 136 @ 1200 mm (Section 1 and 2)
19	Test 18 with lowering of plateau at north and opening of a drainage channel to the sea at 1.5 m MSL	Combination of Box culverts (1200 mm W x 1500 mm H) and 2000 m W x 1500 mm H)	25 @ 2000 mm W @ 15 m centres (Section 2). 136 @ 1200 mm W (Section 1 and 2)
20	Two open piled bridge sections along Section 2, box culverts elsewhere, with lowering of plateau at north	Combination of 200 m bridge sections and Box culverts (1200 mm W x 1500 mm H)	2 x 200 m wide open sections (Section 2) 66 box culverts @ 1200 mm (Section 1 and 2)
21	Four open piled bridge sections along Section 2, box culverts elsewhere, with lowering of plateau at north opening of a drainage channel to the sea at 1.5 m MSL	Combination of 200 m bridge sections and Box culverts (1200 mm W x 1500 mm H)	4 @ 200 m (Section 2) 66 @ 1200 mm (Section 1 and 2)
22	Causeway at 4.2 m, with drop down to natural ground level over 5 sections, with box culverts over some causeway sections.	Flood-ways (200 m long) Box culverts (1200 x 1500 mm high)	5 @ 200 m (Section 1 & 2) 7 box culverts @ 1200 mm (Section 2 only)

3.5 Environmental forcing

Environmental forcing of the model was imposed by variations in tidal level along the offshore boundary of the nested model domains. Previous assessment documented in RPS (2019) provided validation that tides were correctly propagated into the tidal creeks by the model. Consistent with forcing applied to assess inundation over the wider project area (RPS, 2019), a sample period of tidal variation was selected covering a spring tide period over which peak heights ranged from 1.4 m above MSL to 2.2 m above MSL (2nd January to 10th January 2018). There are marked inequalities in high and low tide levels over the study

region, and the initial tests were conducted over a period with 2 relatively high peaks (2 m and 2.2 m) with lower peaks (1.6 and 1.75 m) between. The final comparison between the base case and the optimal design covered this period and an additional low (1.8 m) and high peak (2.3 m).

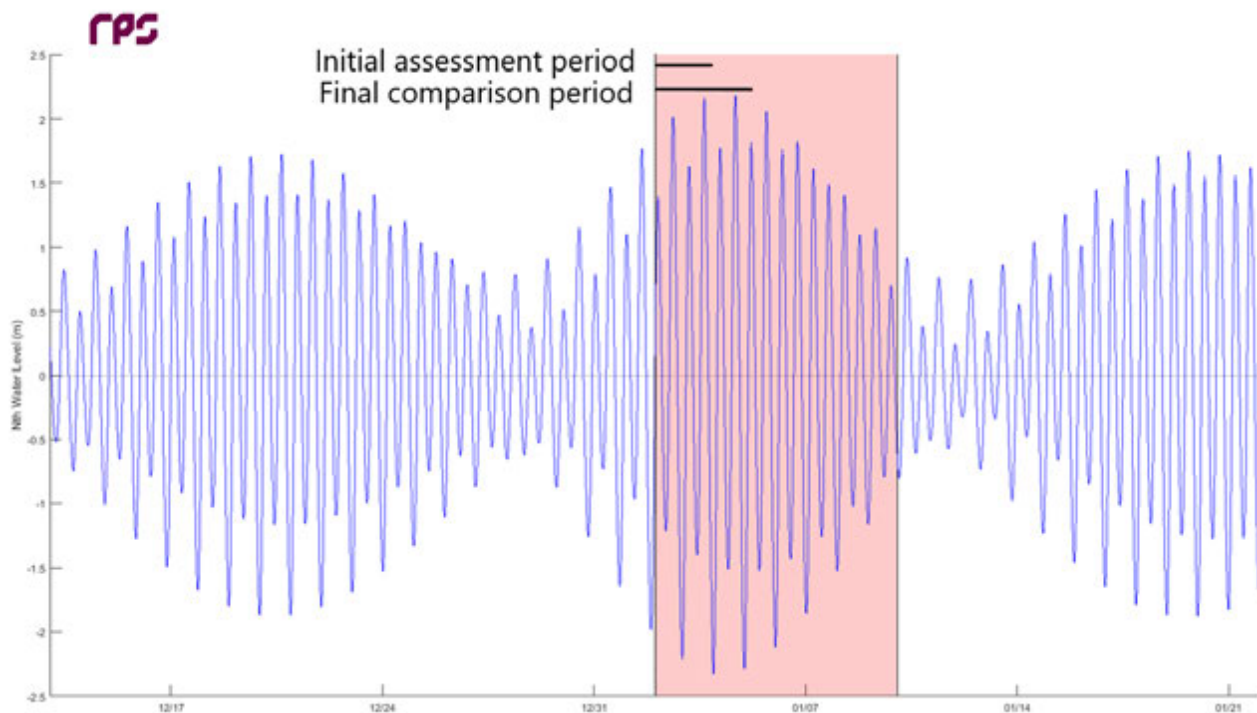


Figure 3.5 Sample tidal variation along the northern portion of the grid that was applied to the assessment. The pink box defines a period of high spring tides. The black lines bracket the period applied to initial tests and for the subsequent comparison.

3.6 Observation points - – Comparative inundation for optimum design

For the final comparison of the Base Case and the optimal causeway design, observation points were defined by BCI for comparison of inundation depth over the tidal sequence. BCI defined 7 sites (AME1-7) within the mapped distribution of algal mats on the inland side of the proposed causeway alignment. A further observation site (AME8) was defined for a site that supports samphire habitat.

The location of sites is shown in Figure 3.6

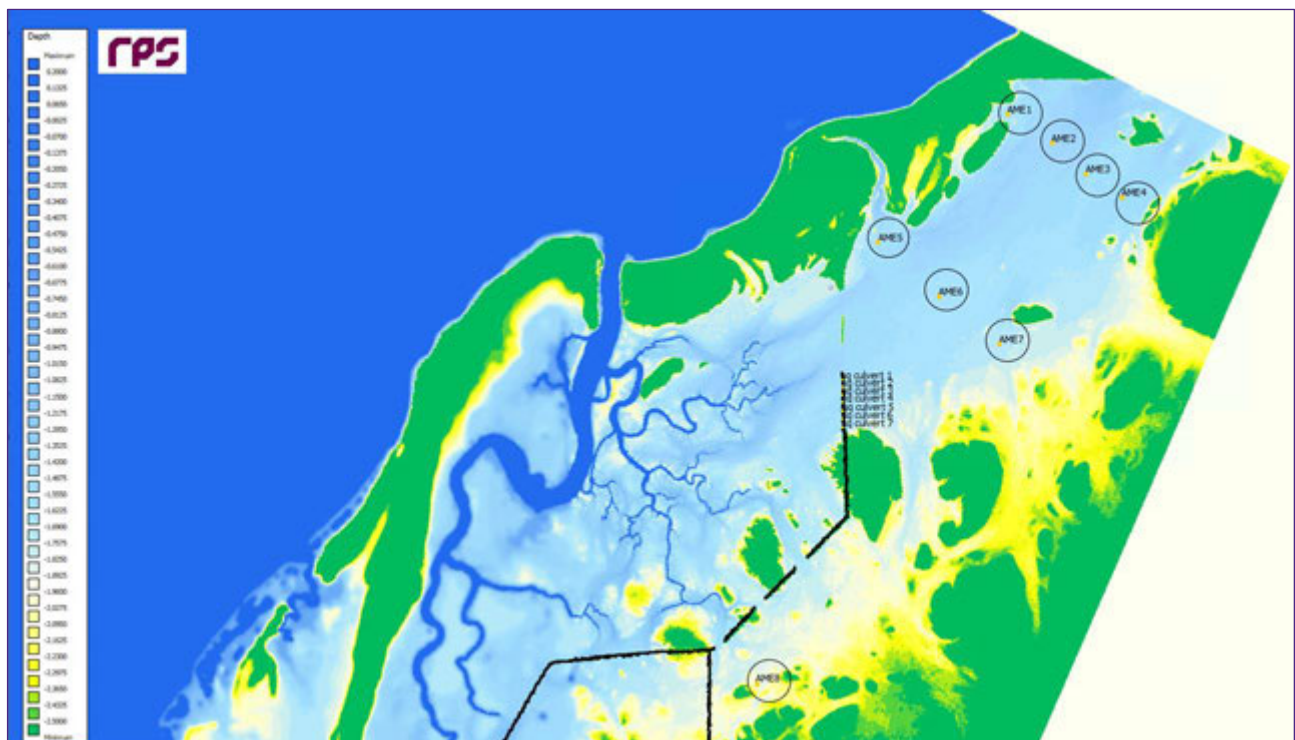


Figure 3.6: Design of the causeway represented by Test 22. The black lines represent sections that are 4.4. m above MSL. The green line along Section 2 represents a section along the causeway that is set at 2.5 m MSL. Elsewhere, the natural topography is preserved. Locations marked Sq. culvert have 1.5 m wide square culverts set at ground level penetrating the raised section of causeway. Observation points for water inundation (AME1-8) are plotted.

3.7 Initial testing for variations of culverts and causeway heights

Simulation over the natural topography and without a causeway or ponds in place indicated that inundation over parts of the clay-pan beyond the causeway alignment would occur with a relatively low spring tide level, as indicated by flooding that was triggered by the first 1.4 m tidal peak. The simulation indicated that water would flood out from the sides and ends of the creek to form a shallow lake that flowed as a wide sheet. This sheet flow would build up momentum as the tidal height offshore reached the peak and the front of the sheet-flow would continue to flow into the claypan while the water at the back of the flow would begin to retard and flow back towards the creeks. A ridge of marginally higher ground is present immediately inland from the proposed causeway alignment and water that flows over this ridge sheets out over the lower land beyond. The combination of the timing of the floods relative to the peak tide and the effect of the ridge in accelerating water inland if the water passes over the ridge appears to be the driver of the wider sheet flow.

These effects are magnified during higher spring tides, as indicated by the simulation period covering the 2nd and 4th spring tidal peak. The sheet flow over these higher peaks was deeper, in general, wider and penetrated further along the clay-pan. The front of the flood arrives at a similar time across the width of the clay-pan but accumulates to deeper depths (25-40 cm) beyond the ridge along the path where the ground level is 15-30 cm lower.

Simulations of most of the test cases for drainage through the proposed Causeway indicated marked impairment of inundation over the clay-pan beyond the alignment. Plots showing the area that was inundated and the depth of water at the peak of the inundation flood for each test case are provided in Appendix A.

The impairment of inundation was greatest for configurations that presented relatively low cross-section to flow, compared to the wide area of shallow surface flow across Section 2. Simulations using box culverts generally performed better than those using round pipes, relative to the number of conductors involved, because the depth of the sheet flow would result in water levels that reach only the lower sections of the pipes, which present a low proportion of the available surface area in their lower sections. Increased

inundation was also indicated for simulations that included a larger number of pipes or box culverts. However, even those configurations that involved many pipes or box culverts alone, and might be impractical and over-expensive to construct, did not result in inundation that was comparable to the natural inundation case. The general outcome of these tests was that the rapidly advancing flood accumulated on the seaward side, which stopped the momentum of the sheet flow. Most of the water volume that built up on the seaward side of the causeway in these cases subsequently flowed back towards the creeks as the tide dropped within a short period of the flood pooling against the causeway. This effect is illustrated in Figure 3.9 for Test 15, which involved the largest number of box culverts. The sequence that is illustrated is for the second, higher, tidal peak (2.2 m) after the smaller tidal peak has occurred and can be compared with the sequence in Figure 3.8

Those configurations that resulted in similar levels of inundation over both the low and high spring peaks included large openings that were concentrated along the lower ground that would carry the larger proportion of the flood volumes and maintain the momentum of the flood over the ridge that lies inland of the causeway alignment. Test 4 that included multiple open bridge sections, including sections 200 m and 30 m wide, and multiple 10 m wide openings at regular centres produced inundation comparable to the natural inundation. Test 5, which was a variation on Test 4 with inclusive of drains dug along the causeway alignment also indicated that inundation comparable to the Base Case would be achieved. However, these cases would involve very high costs of construction and Test 5 would require extensive ground-works to construct the ditches, with other potential for disturbance.

Test 18, 19 and 21 that represented alternative flow structures through the causeway in combination with trenching of a natural drainage ditch to connect this directly to the sea (tide-height dependent: set at 1.5 m AHD in the simulations) in order to encourage seawater to enter the clay-pan directly on the landward side of the causeway alignment, by-passing the dependence on flow through the causeway, resulted in deeper flood depths being calculated over a relatively narrow section of the claypan, corresponding to the lower sections. The wider path of the sheet flood indicated in the Base Case was not reproduced. It was also noted that there was a time-offset between the arrival of flooding tidal levels at the coast and at the claypan behind the creeks, resulting in a marked change in the frequency and durations of the floodwater over the clay-pan. Adjustment of the height of the channel might allow for tuning of the inundation pattern but this option was subsequently dismissed by BCI over concerns for other secondary effects, including potential environmental effects at the discharge location and altered exchange of water between the mangroves, saltmarsh and crusting-algal communities.

Test 20, which would involve construction of an extensive number of bridges supported on piles, which would be at higher costs and would carry higher risks of altering local topography during construction, resulted in relatively high flow depths along the deeper parts of the clay-pan occupied by the algal mats but lower coverage of inundation than the Base Case.

One case that best reproduced the inundation patterns calculated for the Base Case was Test 22, which involved opening the causeway to natural flows over five, 200 m wide, flood-ways along Section 1 and 2, supplemented by additional box culverts over one part of Section 2 and lowering of a high plateau at the northern end of the alignment. The flood-ways were placed across the lowest ground sections to avoid reduction of the momentum of the sheet flow for the largest volume of water entering across Sections 1 and 2. This configuration was considered the most practical option with the least potential for other secondary impacts and was carried forward into the next phase of the comparison.

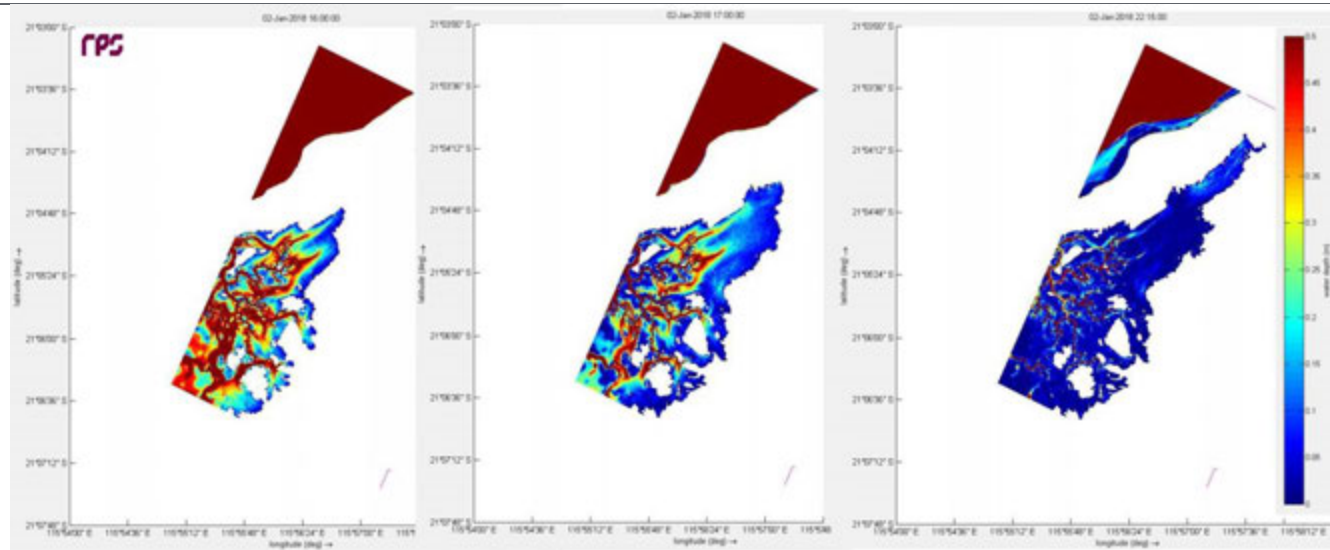


Figure 3.7: Calculations for local water depth over the focus area (natural topography) during a relatively low (1.4 m) spring tide. Time differences between the images are 1 hour and then 5 hours.

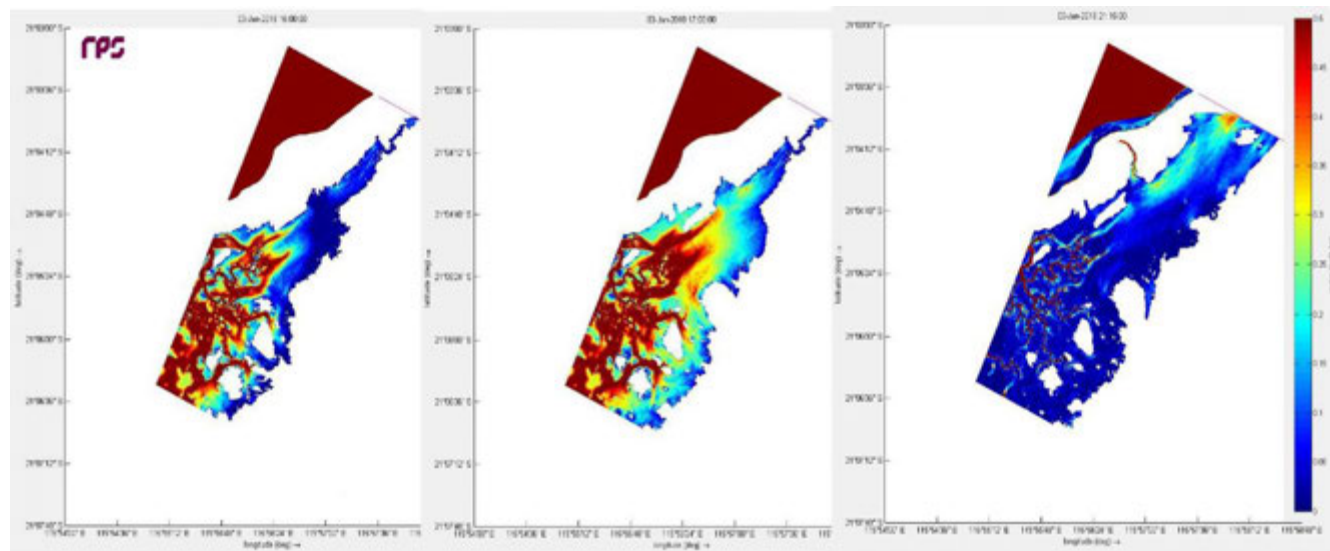


Figure 3.8: Calculations for local water depth over the focus area (natural topography) during a relatively high (2.2 m) spring tide following the lower tidal peak shown in Figure 3.7. Time differences between the images are 1 hour and then 5 hours.

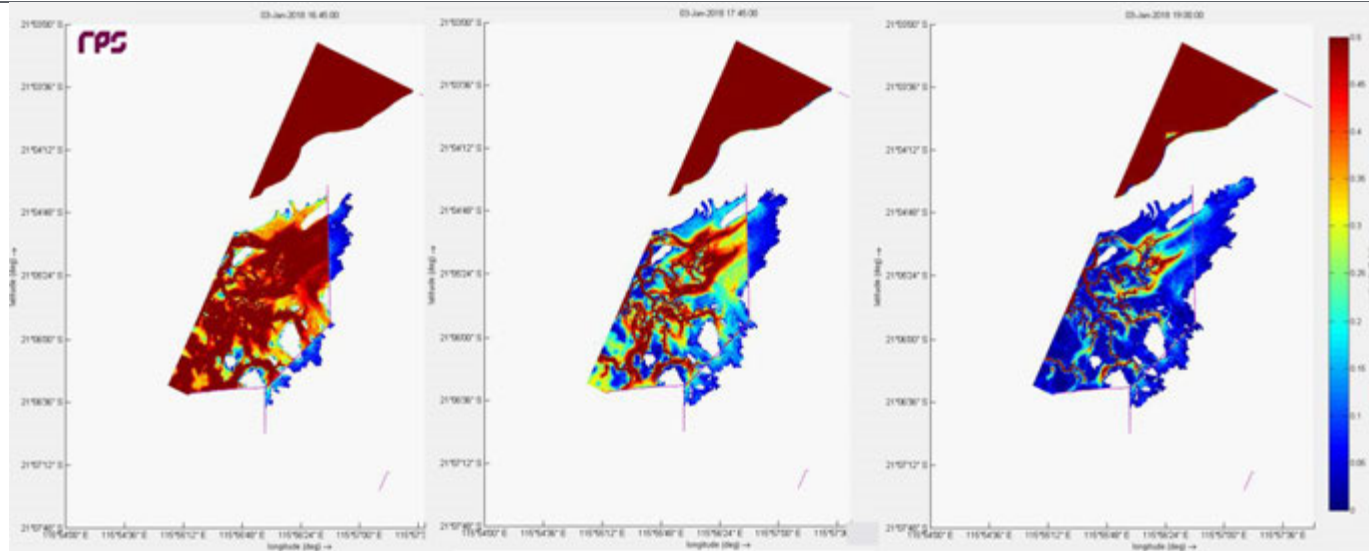


Figure 3.9: Calculations for water depth over the focus area with the causeway in place and with the opening structures specified for Test 15 (See Table 3-1) over the period of a relatively high (2.2 m) spring tide following the lower tidal peak.

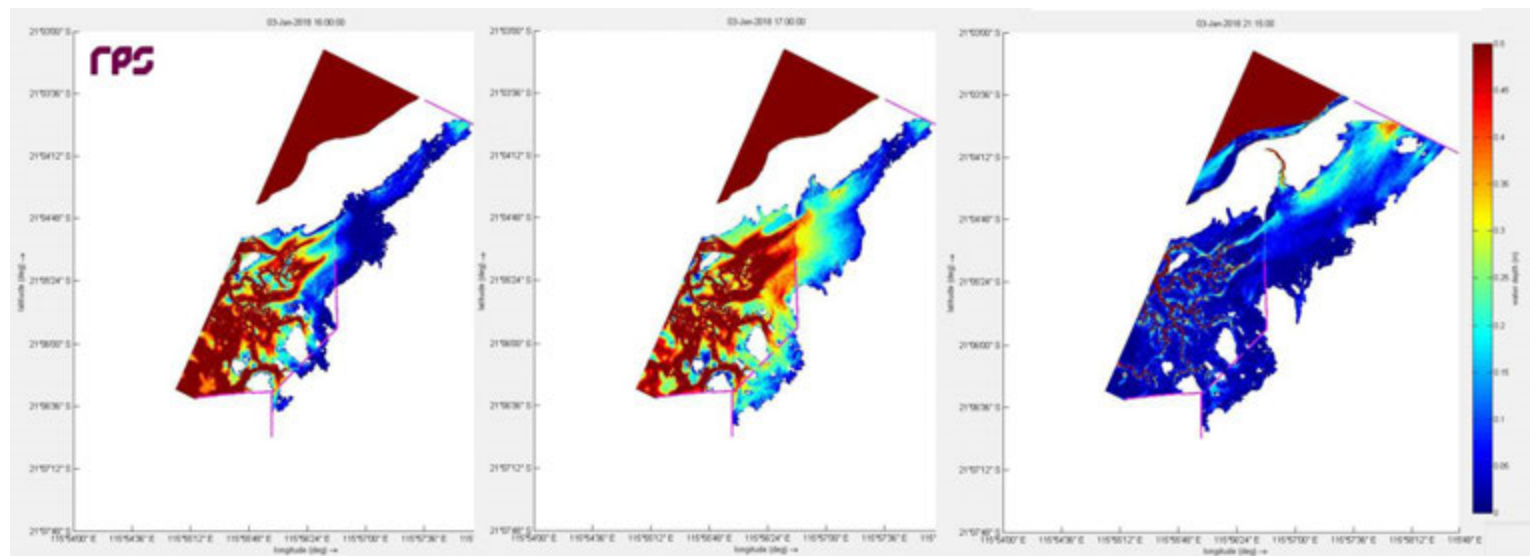


Figure 3.10: Calculations for water depth over the focus area with the causeway in place and with the opening structures specified for Test 22 (See Table 3-1) over the period of a relatively high (2.2 m) spring tide following the lower tidal peak.

3.8 Comparison of inundation over full spring tide for optimum design

Hydrographs, representing local water depth over time calculated for all observation locations (AME 1-8 in) were similar (within 1 cm) for the base case and causeway configuration represented by Test 22 (Figure 2.1) indicating that similar volumes of water should be conducted into, and out of, the habitats behind the causeway alignment, with the modifications represented by Test 22. Water depths calculated for all locations are relatively low (~ 22 cm maximum at AME 5) with peak heights occurring for only short periods of time (minutes).

These hydrographs represent water depth variation over a sequence where 5 tidal peaks inundated parts of the clay-pan, including observation points AME 5 and 6 but other observation points were inundated over only 3 of the major peaks in the Base Case. The same peaks were calculated for Test 22.

The phase of the inundations was also identical for all observation points indicated that there would be no change in the period or timing of wetting of the algal habitats on the clay-pans.

AME6, which is located along the major floodway received slightly more water at the start of the first spring pulse in the Rev 22 case. This may result from the lowering and reshaping of the plateau at the northern end, directing more water into the flood-ways that were aligned with this observation point.

Flooding over all sites is calculated to occur faster than ebbing, in both the natural case and for Test 22 configuration, which can be attributed to the larger effect of the offshore tidal head on pushing the flood waters over the ridge on the inland side of the causeway alignment. Drainage would occur through gravity acting on the held-up water to push water back over the ridge. Ebb flow for the larger flood peaks is faster initially for the period where the flood level is higher than the ridge and then slows as the water level approaches the relative height of the ridge and the model indicates that some water would pool on the inland side of the ridge in both the Base Case and Test 22.

Lower water depths were calculated (for both the Base Case and Test 22) at the end of the ebb-phases between spring tide peaks at the observation points that were positioned along the lower ground levels closer to the causeway alignment (e.g. AME 5 AME 6) than at the back of the clay-pan (e.g. AME 2, 3 and 4). The higher accumulation at the back of the claypan is attributed to pooling over sections of lower ground. Other processes not included in the model, including evaporation, and percolation into the ground are expected to result in lowering of held-up water depths over longer time-scales (i.e. over the subsequent neap-tide sequence). The volume shown to be trapped in the calculations (both Base Case and Test 22) over the spring tidal sequence may also be overstated by the model because the topographic scale of the model cannot represent very small (i.e. 10s of cm to a few m wide) drainage paths that are likely to be present across the claypan due to erosion.

Overall, we conclude that the design of the causeway represented by Test 22 should support maintenance of natural inundation patterns and exchange of water between the mangrove, saltmarsh and crusting algal habitats at the northern end of the Mardie Development Area.

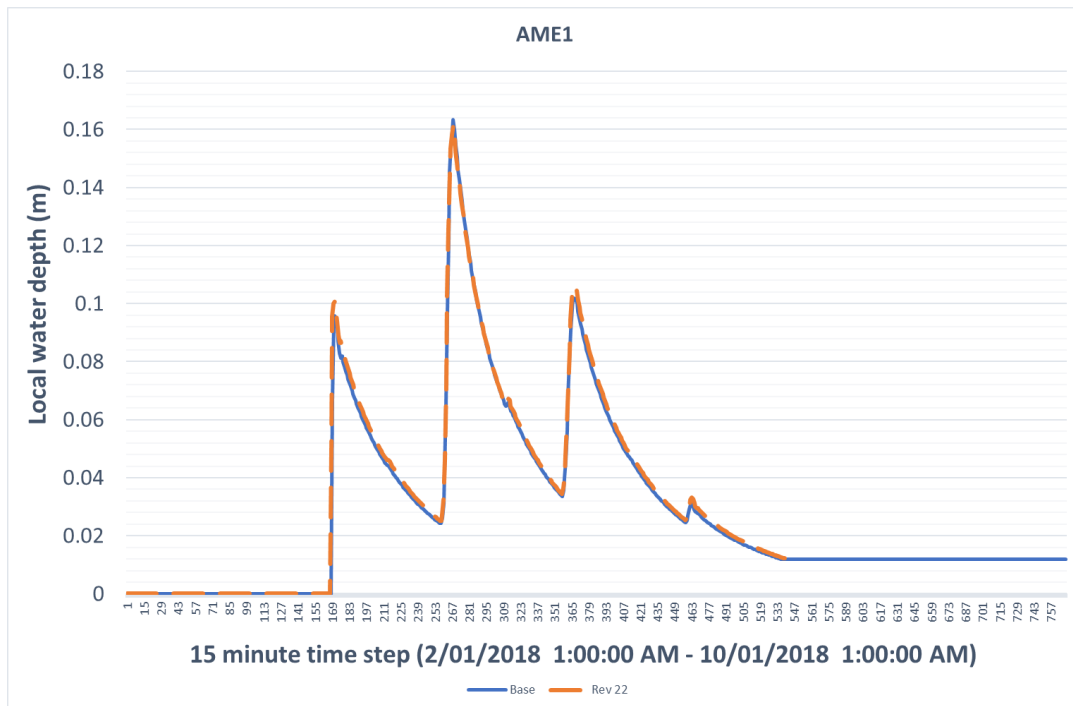


Figure 3.11 Local water depth over time at AME1 comparing the Base Case (blue line) and Test 22 configuration (orange dashed line). See Figure 3.6 for location.

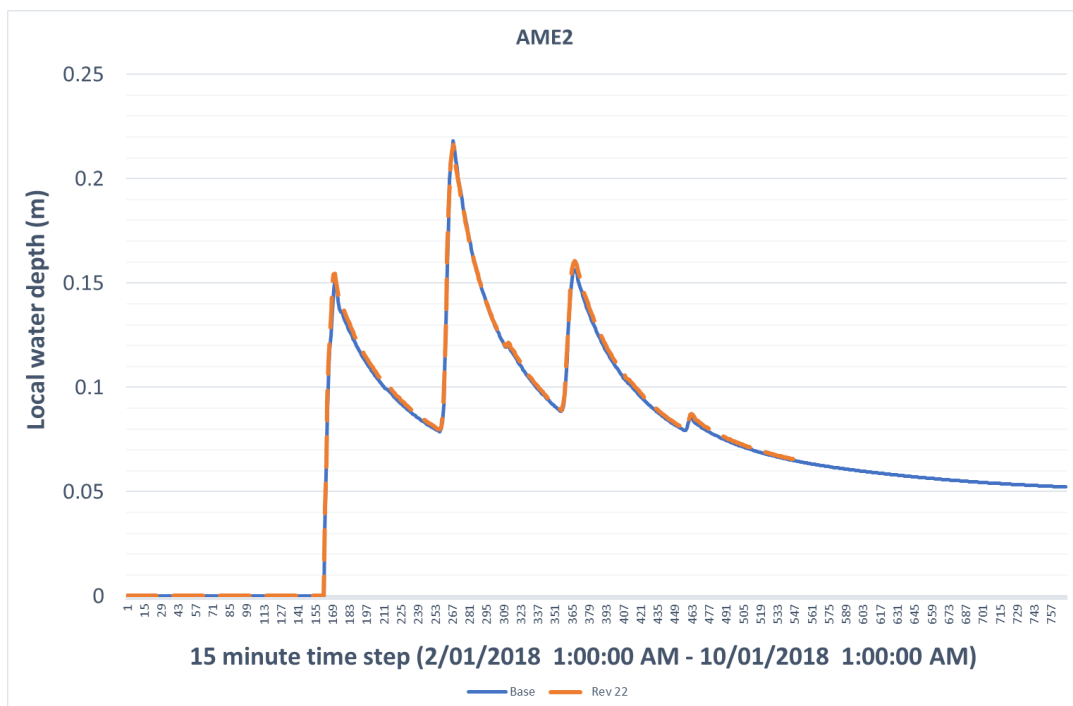


Figure 3.12 Local water depth over time at AME2 comparing the Base Case (blue line) and Test 22 configuration (orange dashed line). See Figure 3.6 for location.

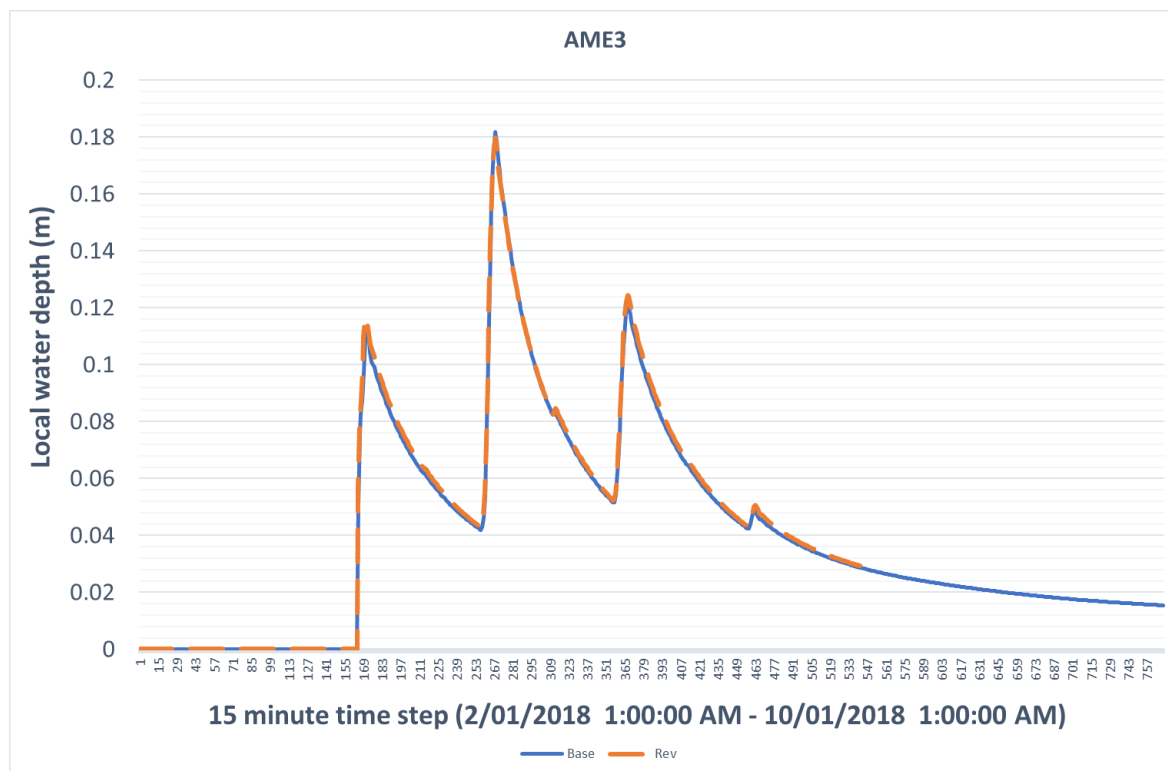


Figure 3.13 Local water depth over time at AME3 comparing the Base Case (blue line) and Test 22 configuration (orange dashed line). See Figure 3.6 for location.

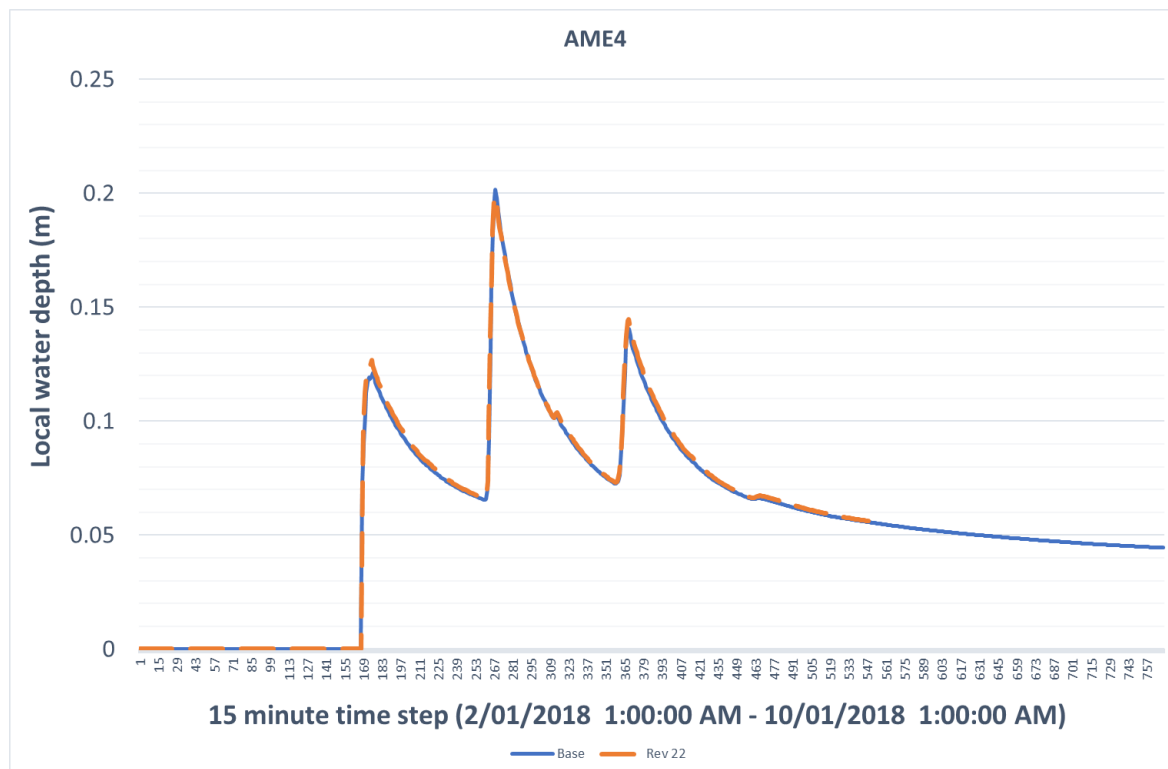


Figure 3.11 Local water depth over time at AME1 comparing the Base Case (blue line) and Test 22 configuration (orange dashed line)

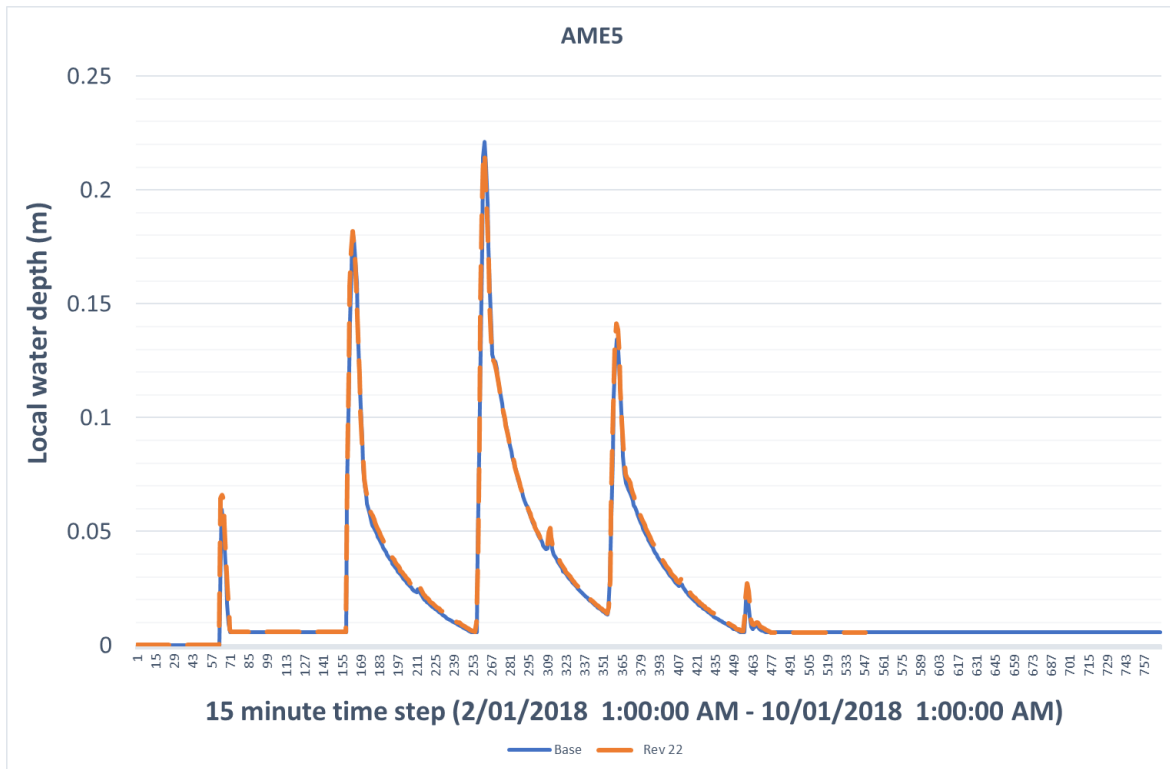


Figure 3.14 Local water depth over time at AME5 comparing the Base Case (blue line) and Test 22 configuration (orange dashed line). See Figure 3.6 for location.

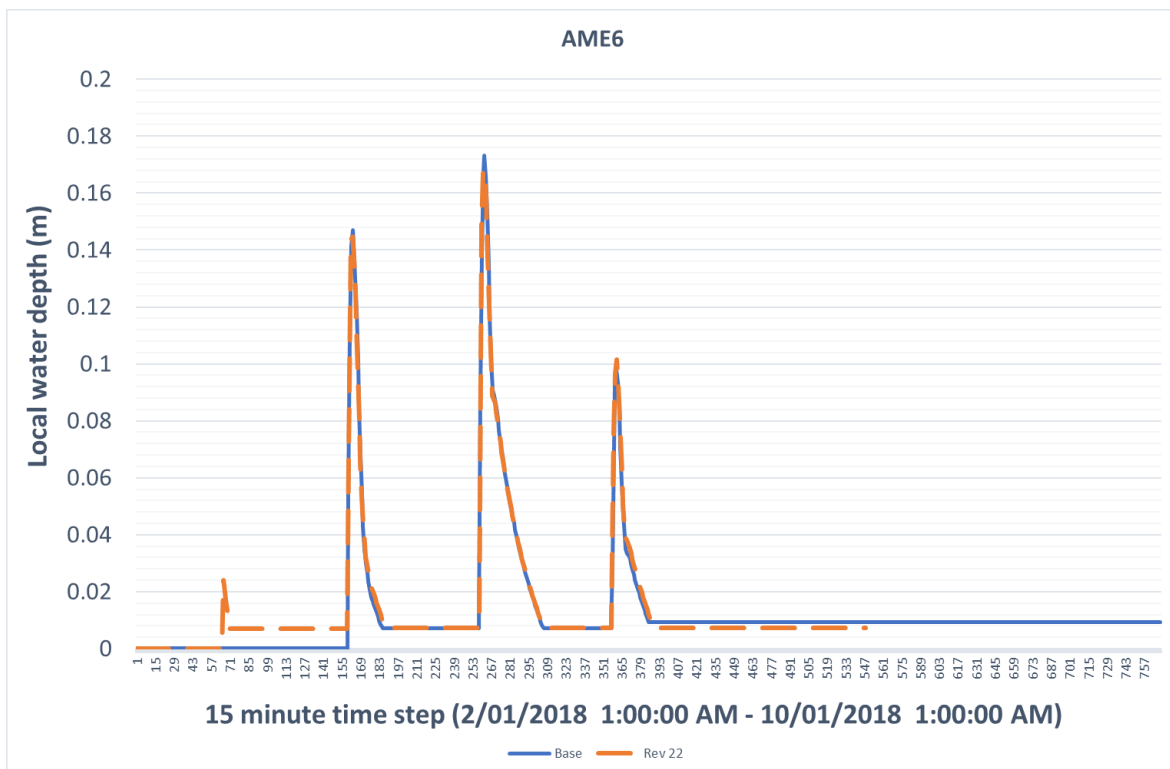


Figure 3.15 Local water depth over time at AME6 comparing the Base Case (blue line) and Test 22 configuration (orange dashed line). See Figure 3.6 for location.

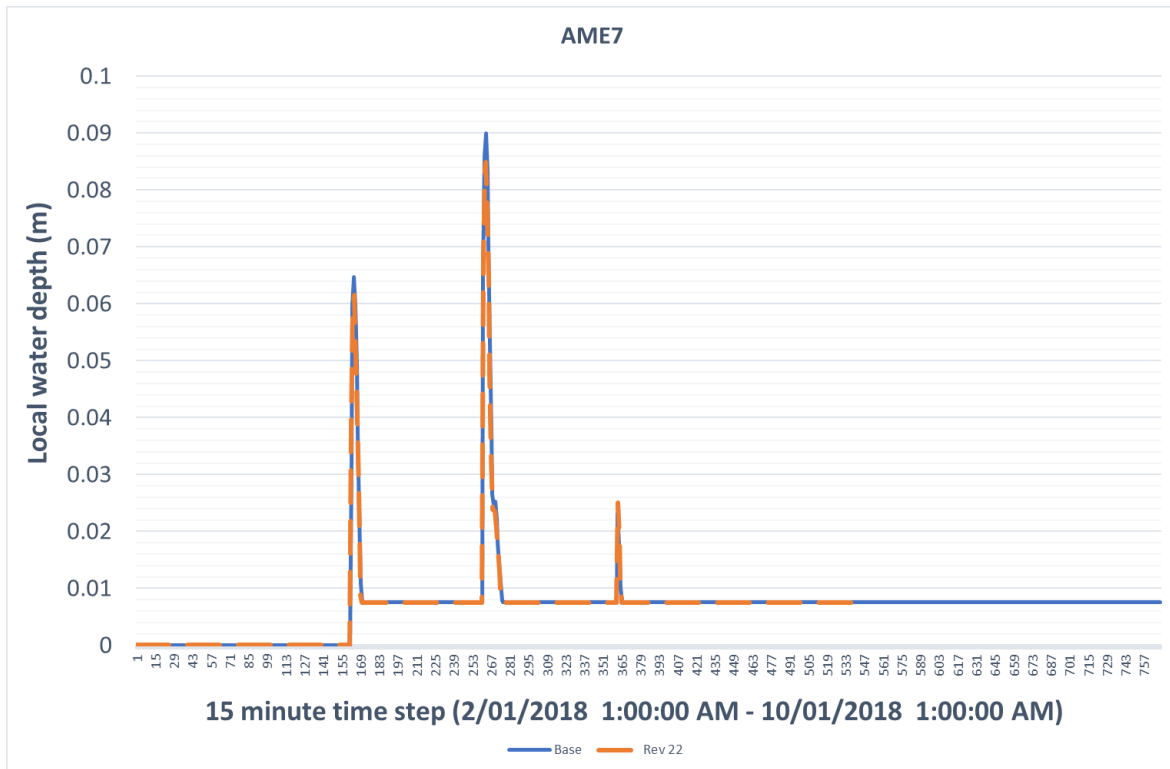


Figure 3.16 Local water depth over time at AME7 comparing the Base Case (blue line) and Test 22 configuration (orange dashed line). See Figure 3.6 for location.

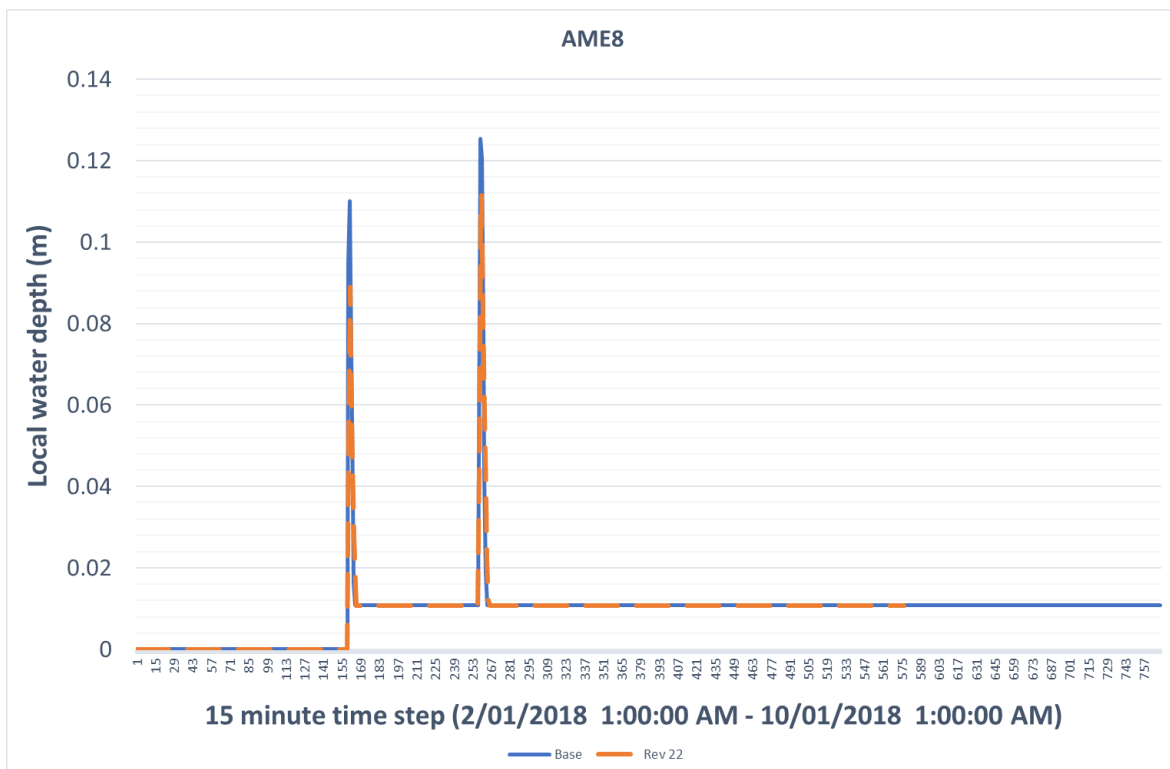


Figure 3.17 Local water depth over time at AME8 comparing the Base Case (blue line) and Test 22 configuration (orange dashed line). See Figure 3.6 for location.

4 REFERENCES

RPS (2019) MAW0616J.006 BCI Mardie Salt Project Report for revised ponds (Rev 3). Report to BCI Minerals,.

Appendix A:

Plots showing inundation and local water depth calculated over the focus area for the Base Case and Test Cases.

The calculations are for the peak flood times at the end of the second, higher, tidal peak (2.2 m MSL) in each case.

